Journal of Thermal Analysis and Calorimetry, Vol. 72 (2003) 657–666

STUDY OF THE CRYSTALLIZATION AND MELTING REGION OF PET AND PEN AND THEIR BLENDS BY TMDSC

S. Montserrat[*]*, F. Roman and P. Colomer*

Departament de Màquines i Motors Tèrmics, Universitat Politècnica de Catalunya,
Carrer de Colom 11, 08222 Terrassa, Spain

Abstracts

The cold crystallization and melting of poly(ethylene therephthalate) (PET), poly(ethylene 2,6-naphthalene dicarboxylate) (PEN) and their blends were studied using temperature modulated differential scanning calorimetry (TMDSC) at underlying heating rates of between 1 and 3 K min^{-1} and periods ranging from 30 to 90 s. The amplitude of modulation was selected in order to give an instantaneous heating rate $\beta \geq 0$.

Heat flow is analyzed by the total heat flow signal ϕ, which is equivalent to the conventional DSC signal, and the reversing heat flow ϕ_{REV}, which only detects the glass transition and the melting processes. The dependence of the melting region in the reversing heat flow on the frequency of modulation is analyzed. The use of the so-called non-reversing heat flow ϕ_{NREV} ($=\phi-\phi_{REV}$) and the effect of frequency and amplitude on the complex heat capacity are also studied. The results show the complexity of these magnitudes.

Keywords: blends, crystallization, melting, PEN, PET, TMDSC

Introduction

In recent years the study of the thermal properties of poly(ethylene 2,6-naphthalene dicarboxylate) (PEN) and its blends and copolymers with poly(ethylene terephthalate) (PET) have received special attention due to the commercial interest and the engineering applications of these polymers. Many studies have been performed using differential scanning calorimetry (DSC). Wunderlich *et al*. [1] described the melting region of PEN through measurements of its heat capacity, Zachmann *et al*. [2] characterized the two crystal forms of PEN by DSC and wide X-ray scattering and Sauer *et al*. [3] studied the presence of multiple endotherms in PEN due to the melting and re-crystallization processes.

The introduction of temperature modulated differential scanning calorimetry (TMDSC) during the last decade [4, 5] allows the study of new aspects of the crystallization-melting region, and specifically those related to the structure and morphol-

* Author for correspondence: E-mail: montserrat@mmt.upc.es

1388–6150/2003/ $ 20.00
Akadémiai Kiadó, Budapest
© 2003 Akadémiai Kiadó, Budapest
Kluwer Academic Publishers, Dordrecht

ogy of these polymers. Recently, TMDSC has been used to study the thermal properties of PEN and its blends with PET [6] showing some of its advantages over conventional DSC. While TMDSC does provide new insights into the study of melting and re-crystallization, on the other hand it causes some of the thermal magnitudes to be dependent upon both the period and amplitude of the modulation, which complicates the interpretation of these properties.

The objective of this work is to study the crystallization and melting region of PET, PEN and their blends using TMDSC and to show what new information can be obtained in comparison with conventional DSC study.

Experimental

Materials and sample preparation

The samples were films of poly(ethylene terephthalate) (PET) and poly(ethylene 2,6-naphthalene dicarboxylate) (PEN). Blends of PET/PEN (90/10 and 70/30 mass/mass) were prepared by melt extrusion at 290ºC for 5 min, using a Haake Rheocorder twin screw extruder. From the extruded samples, films of approximately 0.5 mm thickness were obtained by melting at 290ºC for 5 min under 130 bar of pressure and quenched to room temperature using a Collins press. The films containing pure components were molded under the same conditions. Small pieces of these films of about 5–6 mg were enclosed in aluminium pans for calorimetric analysis.

Calorimetric measurements

The temperature modulated DSC analyses were performed using a Mettler Toledo DSC 821e equipped with an intracooler accessory. The results were evaluated with the alternating DSC (ADSC) application of the STAR^e software. All necessary blank and calibration measurements were performed before measuring the sample in order to ensure optimum results. The non-isothermal ADSC curves were performed with $\tau_{lag}=0$. A nitrogen gas flow of 50 mL min^{-1} was used.

ADSC is a temperature modulated DSC technique, commercialized by Mettler Toledo whose fundamental aspects have been shown and discussed elsewhere [7, 8]. ADSC is based on the superimposition of a sinusoidal varying temperature on the linear heating rate: $T=T_0+\beta_0 t+A_T\sin(\omega t)$, where T_0 is the initial temperature, β_0 is the underlying (or average) heating rate, and A_T and ω are, respectively, the amplitude and the radial frequency of the modulation. The instantaneous heating rate β is described by $\beta=\beta_0+A_T\omega\cos(\omega t)$.

In the case of crystallization and melting, the use of positive instantaneous heating rates ($\beta\geq 0$) is recommended in order to avoid an extra crystallization. This condition is achieved in the following relation of the modulation parameters:

$$A_T = \frac{\beta_0\,(\mathrm{K\ s^{-1}})}{2\pi/\,p(\mathrm{s})} \qquad (1)$$

where p is the modulation period. For an underlying heating rate β_0=2 K min^{-1}, the condition $\beta \geq 0$ is fulfilled for the following pairs of values of A_T and p: 0.159 K and 30 s, 0.318 K and 60 s, or 0.477 K and 90 s.

The modulation of the heating rate gives a modulated heat flow signal, ϕ. The Fourier analysis separates this signal into different components:

i) The total heat flow ϕ, which is equivalent to the heat flow obtained by conventional DSC at the same heating rate β_0.

ii) According to Schawe's approach [9], based on the linear response theory, a complex heat capacity C_p^* is defined ($C_p^*=C_p'-iC_p''$), whose modulus is determined by the ratio of the amplitudes of the heat flow A_ϕ and the heating rate A_q.

The real and imaginary parts of C_p^* are respectively defined by

$$C_p' = |C_p'| \cos\delta \tag{2}$$

$$C_p'' = |C_p'^*| \sin\delta \tag{3}$$

where δ is the phase angle between the modulated heat flow and the heating rate, which detects the relaxation processes during the ADSC experiment.

Alternatively, the reversing and non-reversing heat flow approach introduced by Reading and co-workers [4, 5, 10] defines the reversing heat flow ϕ_{REV} by the product $-C_p'\beta_0$. In the glass transition region the phase angle is small, $\cos\delta \approx 1$ and C_p' is practically equal to the modulus $|C_p^*|$. The non-reversing heat flow ϕ_{NREV} is defined as the difference between total heat flow and reversing heat flow signals.

Results and discussion

Heat flow signals in the crystallization and melting region

Heat flow signals obtained in PET at β_0=3 K min^{-1}, an amplitude of 0.2 K and a period of 50 s are shown in Fig. 1. The total heat flow shows the glass transition region between 60 and 90ºC with a sub–T_g peak due to the physical ageing of the sample at room temperature [11]. There follows an exothermic peak between 110 and 140ºC which corresponds to the cold crystallization of the PET, and an endothermic peak between 230 and 270ºC in the region of the melting process.

The enthalpies of crystallization and melting obtained by separate integration of the areas are –33.3 and +54.6 J g^{-1}, respectively. The addition of these values gives an endothermic value of 21.7 J g^{-1}, which could be attributed to the melting of the initial crystallinity content of the sample. Nevertheless, the recommended method for calculating the crystallinity [12] consists of integrating both areas by means of a single baseline from the beginning of the cold crystallization peak to the end of the melting peak. This procedure yields an endothermic value of +18.5 J g^{-1}. Assuming an estimated heat of melting of 140 J g^{-1} for 100% crystalline PET, a crystallinity of 13.2% is calculated. According to other authors [13, 14], the total heat flow gives practically the same information as that obtained by conventional DSC, and the position of the

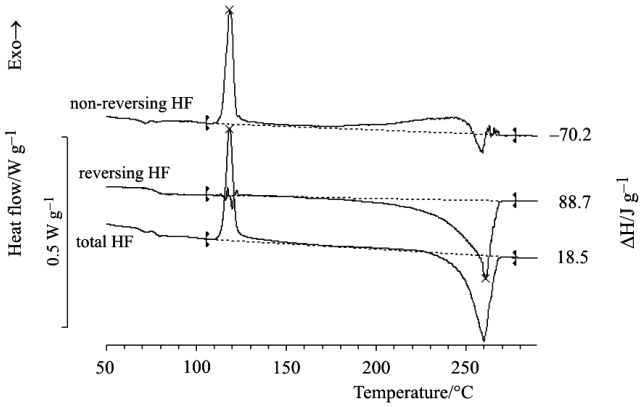

Fig. 1 Total heat flow, reversing heat flow and non-reversing heat flow of a film of PET, obtained at an underlying heating rate of 3 K min^{-1}, an amplitude of 0.2 K and a period of 50 s. The values of the integration between the beginning of the cold crystallisation (113°C) and the end of the melting (272°C) are also indicated for the different heat flow signals

thermal events depends only on the underlying heating rate (due to limitations of length, these results have been omitted from this paper).

Figure 1 also shows the reversing heat flow ϕ_{REV} obtained from the heat capacity measurement. The ϕ_{REV} signal only shows two thermal events: the glass transition and the endothermic peak of melting.

The glass transition is shown without ageing effects, and differs from the T_g obtained by the total heat flow. The former is the dynamic glass transition, which is frequency-dependent, and the latter is the thermal or conventional DSC, which is heating rate-dependent [8, 14]. The ϕ_{REV} is not sensitive to cold crystallization, although a small oscillation is observed. This oscillation can be attributed to the small number of waves of the modulation during the crystallization, as it disappears when shorter periods are used (e.g. a modulation of 2 K min^{-1}, 0.159 K and 30 s). Above the glass transition ϕ_{REV} only shows an endothermic melting peak with an enthalpy change $\Delta H(\phi_{REV})$=88.7 J g^{-1}, which is larger than that calculated from the total heat flow (58.6 J g^{-1}). In addition, it is observed that the melting starts at about 150ºC, which is about 80ºC before the melting shown by the ϕ signal. The cold crystallization causes a distribution of metastable crystallites, which are submitted to continuous melting and re-crystallization during a non-isothermal process until the melting is completed [15]. This continuous melting is detected by the complex heat capacity and shown by the ϕ_{REV} signal. As the melting and re-crystallization processes depend on the heating (cooling) rate β, it results that the $\Delta H(\phi_{REV})$ is dependent on the modulation conditions. This effect is shown for PET and the PET/PEN 70/30 blend in Figs 2a and 2b, respectively: the longer the period of modulation, the higher the heat of melting as measured by ϕ_{REV}. In the 70/30 blend it is observed that $\Delta H(\phi_{REV})$ for a period of 90 s is much lower than in PET.

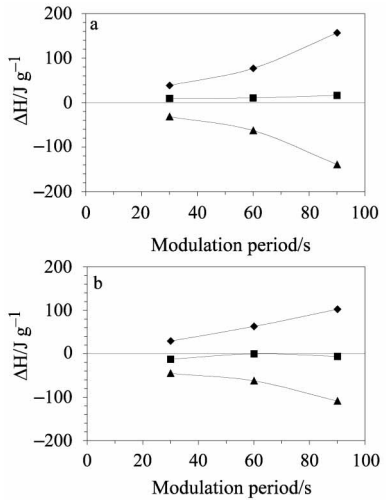

Fig. 2 Effect of the period on the ΔH obtained by ■ – integrating the heat flow, ◆ – reversing heat flow and ▲ – non-reversing heat flow in a – PET and b – PET/PEN 70/30. The underlying heating rate was 2 K min^{-1}, and the amplitude was selected in order to give an instantaneous heating rate $\beta \geq 0$: 0.159 K for 30 s, 0.318 K for 60 s, and 0.477 K for 90 s. The dashed lines are a guide for the eye

The PET/PEN 70/30 blends show a unique peak of crystallization and melting as a consequence of the transesterification reaction [16]. This reaction creates a block copolymer which in the case of a 70/30 mass ratio yields an average length of PET and PEN sequences of 14.7 and 5.3 units respectively, and a degree of randomness of 0.26. These values were obtained by H NMR. As a result of the presence of PEN units in the copolymer structure, the ΔH of melting observed in the ϕ_{REV} signal of PET/PEN 70/30 is lower than in PET. At the same time, the cold crystallization is retarded and the melting advanced. The ϕ signal in experiments using the same modulation conditions (3 K min^{-1}, 0.5 K and 60 s) shows that the peak temperature of cold crystallization increases from 118ºC in PET to 149ºC in PET/PEN 70/30, whereas the peak melting temperature decreases from 259ºC in PET to 244ºC in PET/PEN 70/30.

Taking into account that ϕ shows the overall variation in heat flow and that ϕ_{REV} yields the heat flow involved in the melting of the initial crystalline as well as re-crystallized material, the difference between these two properties, that is, the ϕ_{NREV}, should evidence the cold crystallization and further re-crystallization process. As ϕ_{NREV} not only shows the exothermic events but also part of the endothermic process, this signal is very difficult to interpret. Moreover, ϕ_{NREV} is a complex magnitude, which is obtained by the difference between the heating rate-dependent ϕ and the frequency-dependent ϕ_{REV}.

Some authors [17] suggest that one of the benefits of ϕ_{NREV} is that it enables the initial crystallinity of the sample to be calculated by adding it to the ϕ_{REV}. Nevertheless, similar results can be obtained directly by integrating the ϕ signal between the same limits as those of the integration of ϕ_{REV} and ϕ_{NREV}. Based on the $\Delta H(\phi_{NREV})$ and

$\Delta H(\phi_{REV})$ values of PET given in Fig. 1, –70.2 and 88.7 J g^{-1} respectively, a value of $\Delta H(\phi)$=18.5 J g^{-1} is obtained, which is the same value determined directly by integration of the ϕ signal.

In this context, the non-reversing heat flow signal does not introduce any new quantitative information, but it helps to visualize the re-crystallization processes between cold crystallization and complete melting. This benefit is shown in the non-reversing heat flow signals of PEN and the PET/PEN 70/30 blend in Figs 3 and 4 respectively.

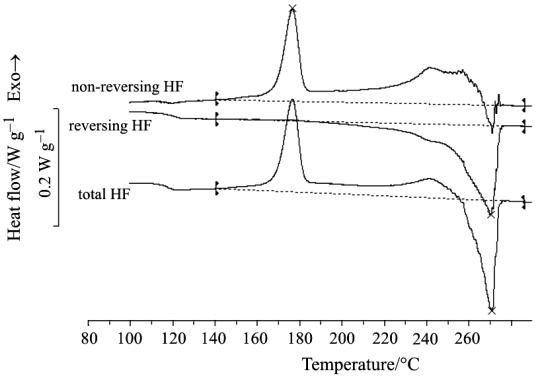

Fig. 3 Total heat flow, reversing heat flow and non-reversing heat flow of a film of PEN, obtained at an underlying heating rate of 2 K min^{-1}, an amplitude of 0.318 K and a period of 60 s

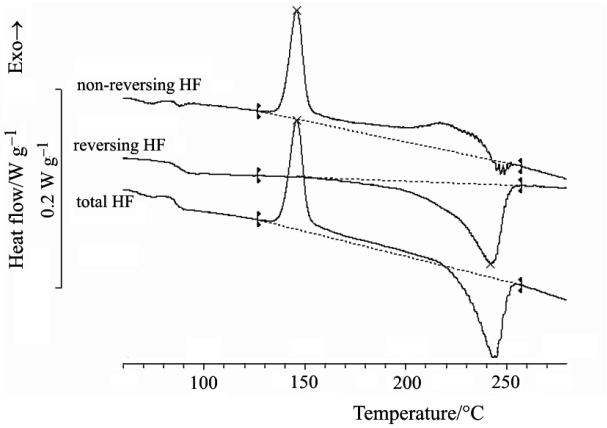

Fig. 4 Total heat flow, reversing heat flow and non-reversing heat flow of a film of PET/PEN 70/30, obtained at an underlying heating rate of 2 K min^{-1}, an amplitude of 0.318 K and a period of 60 s

The total heat flow signal in PEN (Fig. 3) shows a T_g at 117ºC (T_g midpoint), a cold crystallization with a peak temperature of 177ºC, and melting in the range between 240 and 280ºC. A weak exothermic peak is observed at about 240ºC, which is attributed to the crystallization of a second crystalline form [2, 6]. The reversing heat

flow shows melting starting practically at the end of the first peak of crystallization (at about 190ºC). The main melting peak shows a shoulder at about 240ºC, due to the exothermic process of crystallization of the second crystalline form. The non-reversing heat flow shows both crystallizations and the re-crystallization processes up to 260–265ºC. In PEN, TMDSC highlights the presence of two different crystal forms, which have been studied by DSC and X-ray diffraction analysis [2].

In the PET/PEN 70/30 blend, the region between 210 and 220ºC shows a smooth shoulder in the ϕ_{REV} signal, and a flat prominence in the ϕ_{NREV} signal. Although crystallization is mainly due to PET sequences, which comprise the main component, a small co-crystallization effect of PEN is not discarded. Nevertheless, a more detailed study by X-ray analysis should be used to elucidate this effect.

Complex heat capacity during crystallization and melting

The complex heat capacity $|C_p^*|$ and the in-phase component C_p' obviously show the same thermal events as the reversing heat flow; i.e. the glass transition and the melting. These signals for a film of PET scanned in the same conditions as in Fig. 1 (3 K min^{-1}, 0.2 K and 50 s) are shown in Fig. 5. At the same time, the out-phase heat capacity C_p'' and the phase angle show the same thermal transitions as $|C_p^*|$ and C_p' (Fig. 6), but an additional oscillation is detected in the cold crystallization region.

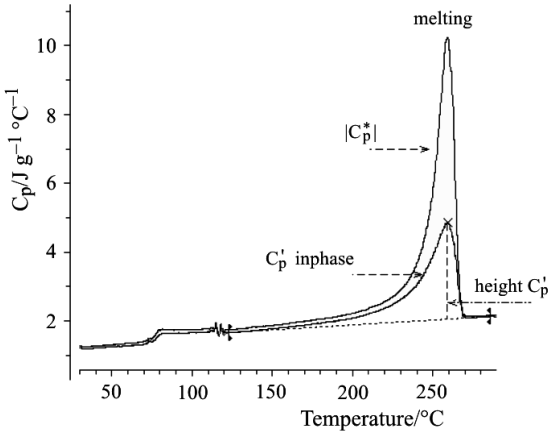

Fig. 5 Complex heat capacity $|C_p^*|$ and in-phase heat capacity C_p' of a film of PET, obtained in the same conditions as in Fig. 1 (3 K min^{-1}, 0.2 K and 50 s). The intensity of the heat capacity is measured by the height of the peak in relation to a baseline as shown for C_p'

The intensity of $|C_p^*|$, C_p' and C_p'' peaks in the melting region depends on the period of modulation, as shown in Fig. 7. This intensity is measured by the height of the peak in relation to a baseline drawn between the beginning and the end of the transition (140 and 280ºC in the case of PET). The results obtained for PET agree with those obtained by Toda *et al*. [18] and Schawe *et al*. [19]. A similar variation of the heat capacity is observed in the PET/PEN 70/30 blend except for the C_p'', which decreases as the period of

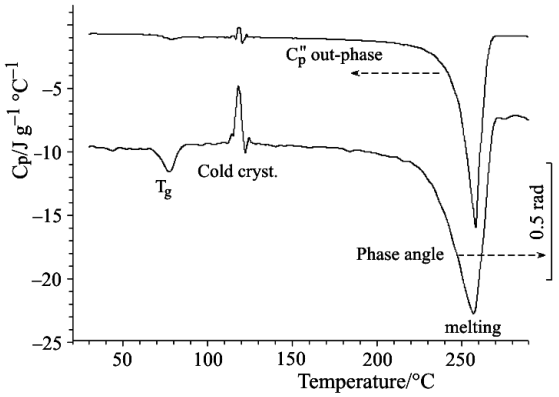

Fig. 6 Out-phase heat capacity C_p'' and phase angle of a film of PET, obtained in the same conditions as in Fig. 1 (3 K min^{-1}, 0.2 K and 50 s)

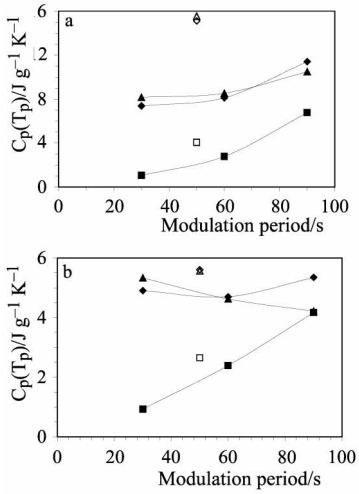

Fig. 7 Effect of period on the intensity of ◆ – $|C_p^*|$,■ – C_p' and ▲ – C_p'' on the peak temperature for PET (a) and PET/PEN 70/30 (b) at an underlying heating rate of 2 K min^{-1}. As in Fig. 2, the amplitude was selected in order to give an instantaneous heating rate $\beta \geq 0$: 0.159 K for 30 s, 0.318 K for 60 s, and 0.477 K for 90 s. The open symbols correspond to the heat capacities measured at 3 K min^{-1}, an amplitude of 0.2 K and a period of 50 s

modulation increases. At the same time, for a similar period of modulation, the intensity of these peaks tends to increase with the underlying heating rate, as shown in Fig. 7 for the modulation 3 K min^{-1}, 0.2 K and 50 s (open symbols).

The dependence of complex heat capacity on frequency has been used by other authors [18–20] to model the kinetics of irreversible melting, but no satisfactory interpretation of this dependence has yet been reached.

The amplitude of modulation also affects the intensity of heat capacity, as shown in Fig. 8 for the 70/30 PET/PEN blend. As the amplitude of modulation decreases the

intensity of heat capacity signals tends to increase. This variation is a consequence of the effect of the maximum (or minimum) heating (or cooling) rate being reached during modulation, which affects the melting and re-crystallization processes. At the lowest amplitude (0.159 K) β_{max}=2 K min^{-1} and β_{min}=0, whereas at the highest A_T the variation of the instantaneous heating rate is about 6 times higher: β_{max}=7.3 K min^{-1} and β_{min}= –5.3 K min^{-1}.

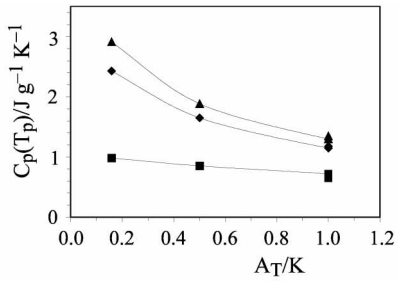

Fig. 8 Effect of the amplitude of modulation on the intensity of ◆ – $|C_p^*|$, ■ – C_p' and ▲ – C_p'' on the peak temperature for PET/PEN 70/30 at an underlying heating rate of 1 K min^{-1} and a period of 60 s

The intensity measured at the peak of $|C_p^*|$ allows one to measure the amplitude of the modulated heat flow at this point:

$$A_\phi(T_p)= |C_p^*|A_q=|C_p^*|\omega A_T$$

Plotting $A_\phi(T_p)$ *vs*. the amplitude of the modulation (Fig. 9) shows a quasi-linear response in the melting region.

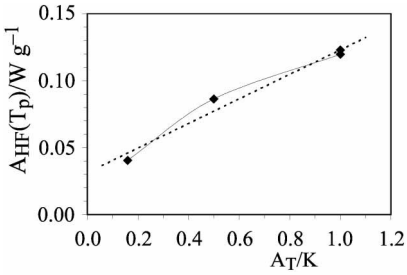

Fig. 9 Variation of the heat flow amplitude at the maximum intensity of $|C_p^*|$ with the amplitude of the modulation of PET/PEN 70/30 at an underlying heating rate of 1 K min^{-1} and a period of 60 s. The dotted line corresponds to the linear fit: $A_\phi(T_p)$=0.0312+0.0919 A_T (r^2=0.972). The dashed line is a guide for the eye

Conclusions

The cold crystallization and the irreversible melting of PET, PEN and their blends is studied by TMDSC. The total heat flow signal ϕ allows the calculation of the crystallinity content as in conventional DSC, whereas the reversing heat flow signal ϕ_{REV} gives addi-

tional information on the multiple melting and re-crystallization processes, which occur during the heating until the melting is completed. The continuous heat of melting measured by this signal $\Delta H(\phi_{REV})$ is dependent on the modulation conditions. The value of $\Delta H(\phi_{REV})$ in the PET/PEN 70/30 blend is lower than in the PET, which is due to the presence of the PEN units in the copolymer structure. In the case of PEN, the ϕ_{REV} signal allows to confirm the presence of two different crystal forms, which have been studied by other authors using DSC and X-ray diffraction analysis [2].

The intensity of the modulus of the complex heat capacity and the in-phase heat capacity increases with the period of modulation in PET and in the blend 70/30. The dependence of the complex heat capacity on the frequency may be used to model the kinetics of the irreversible melting.

* * *

Financial support has been provided by DGI MAT2000-1002-C02-01 and PB98-0921 Projects. The authors acknowledge the technical assistance of the members of the Dep. Física e Ingeniería de Polímeros (ICYTP-CSIC) and Dep. Ingeniería Química (UPC) for the preparation of blends and HRMN characterization, respectively.

References

1 S. D. Cheng and B. Wunderlich, Macromolecules, 21 (1988) 789.
2 S. Buchner, D. Wiswe and H. G. Zachman, Polymer, 30 (1989) 480.
3 B. B. Sauer, W. G. Kampert, E. N. Blanchard, S. A. Threefoot and B. S. Hsiao, Polymer, 41 (2000) 1099.
4 P. S. Gill, S. R. Sauerbrunn and M. Reading, J. Thermal Anal., 40 (1993) 931.
5 M. Reading, D. Elliott and V. L. Hill, J. Thermal Anal., 40 (1993) 949.
6 W. G. Kampert and B. B. Sauer, Polymer, 42 (2001) 8703.
7 J. M. Hutchinson and S. Montserrat, J. Thermal Anal., 47 (1996) 103.
8 S. Montserrat, J. Therm. Anal. Cal., 59 (2000) 289.
9 J. E. K. Schawe and G. W. H. Höhne, J. Thermal Anal., 46 (1996) 893.
10 K. J. Jones, I. Kinshott, M. Reading, A. A. Lacey, C. Nikolopoulos and H. M. Pollock, Thermochim. Acta, 304/305 (1997) 187.
11 S. Montserrat, Progr. Colloid Polym. Sci., 87 (1992) 78.
12 K. H. Illers, Colloid Polym. Sci., 258 (1980) 8.
13 W. Cheng, I.-K. Moon and B. Wunderlich, Polymer, 41 (2000) 4119.
14 J. M. Hutchinson and S. Montserrat, Thermochim. Acta, 377 (2001) 63.
15 B. Wunderlich, Thermal Analysis, Academic Press, New York 1990.
16 T. D. Patcheak and S. A. Jabarin, Polymer, 42 (2001) 8975.
17 E. Verdonck, K. Schaap and L. C. Thomas, Int. J. Pharm., 192 (1999) 3.
18 A. Toda, C. Tomita, M. Hikosaka and Y. Saruyama, Polymer, 39 (1998) 5093.
19 J. E. K. Schawe and E. Bergmann, Thermochim. Acta, 304/305 (1997) 179.
20 A. Toda, C. Tomita and M. Hikosaka, J. Thermal Anal., 54 (1998) 623.